Effect of D-π-A substituted Bromomethylcoumarin Derivatives on Optoelectronic Properties: Experimental and Computational Studies

Mahesh Madar
Department of Physics, V.M.K. S.R.Vastrad College, Hungund
Malatesh S Pujar
Karnatak University Dharwad Department of Physics
Shridhar A H
Department of Chemistry, SVM College Ilkal
Mahantesh M Basanagouda
P C Jabin Science College
Ashok H Sidarai (ashok_sidarai@rediffmail.com)
Karnatak University Dharwad Department of Physics https://orcid.org/0000-0001-5673-4159

Research Article

Keywords: Bromomethylcoumarin, 1BDYMBC, 4BDYMBC, HOMO-LUMO, MESP, Dipole moment

Posted Date: March 29th, 2022

DOI: https://doi.org/10.21203/rs.3.rs-1438743/v1

Abstract

Here we report a simple method for the synthesis of a D–π–A substituted bromomethyl coumarin derivatives 1-(6-Bromo-benzo[1, 3]dioxol-5-yloxymethyl)-benzo[f]chromen-3-one (1BDYMBC) and 4-(6-Bromo-benzo[1, 3]dioxol-5-yloxymethyl)-benzo[h]chromen-2-one (4BDYMBC) via a one-pot chemical reaction. The FT-IR, ^{1}H-NMR, and MS results confirmed the corresponding structure of the synthesized dyes. The substitution effect, on optoelectronic properties was verified using experimental and theoretical techniques. The absorption and fluorescence spectra of fluorescent dyes were recorded in different solvents of different polarity. Stoke's shift exhibits a redshift with an increase in solvent polarity for all molecules indicating a $\pi-\pi*$ transition. The ground state dipole moments of all fluorescent dyes are estimated theoretically from ab initio computations (integral equation formalism of polarizable continuum model) and experimentally from the solvatochromic method and the results are compared. The excited state dipole moments are estimated using solvatochromic correlations equation and results show that the excited state dipole moments are higher than the ground state dipole moments which suggests that, all fluorescent dyes are more polar in the excited state. The HOMO-LUMO energy gaps computed from density functional theory and absorption threshold wavelengths are found to be in good agreement with each other and also support intramolecular charge transfer (ICT). The chemical hardness of the molecules is determined and the chemical stability is discussed. Further, using DFT molecular electrostatic potential (MESP) plots, the electrophilic site and nucleophilic site which are useful in photochemical reactions were identified. Finally, all the preliminary observations and results suggest that the fluorescent dyes can be considered as potential candidates for fluorescent probes and for the construction of dye sensitized solar cell in future.

1. Introduction

Organic optoelectronic materials have been known for almost a century, as the first studies of their optical and electronic properties have been reported in the 1910s. However, a real surge of interest in the field of organic opto-electronics occurred during the past 20 years, due to major improvements in material design and purification that led to a significant boost in the materials performance [1]. Currently, organic materials receiving considerable attention due to their applications in electronic and optoelectronic devices, such as organic thin-film-transistors, light-emitting diodes (OLEDs), solar cells, sensors, photorefractive (PR) devices, and many others. The particular interest in this is because of low-cost, solution-processable thin films, that can be deposited on large areas and/or flexible substrates [2–4].

Coumarin derivatives have attracted substantial interest by their photophysical properties like large optical band gap, high thermal stability, good quantum yield in an extensive of research areas, from their key role in optoelectronics such as solar cell, OLEDs and, photovoltaic. Coumarins are the widespread class of benzopyrone used in academic and industrial sectors as chromophore, pharmacophore, fluorophore, dye sensitizer and they have also been successfully incorporated into energy and electron transfer arrays [5–10].π–conjugated coumarins with enhanced molar absorption coefficient and a third-order nonlinear optical response finds applications in organic photovoltaics as metal-free dye sensitizers, optical communication and optical power limiters respectively. In the recent past, various researchers are trying to evaluate the nonlinear optical properties of coumarin derivatives including optical switching, optical limiting, etc., by designing and tailoring the substituents [11]. Along with optoelectronic properties coumarin derivatives are also exhibits interesting biological, pharmacological, biochemical, therapeutic, and photochemical properties with a wide range of applications [12–13]. Some 4-Aryloxymethyl coumarins are said to be showing antimicrobial activity, lengthy variety coupling and centrosymmetric nature [14–15]. Recently, it's been said that iodinated 4-aryloxymethyl coumarins which include 4-(4-iodophenoxymethyl)-benzo[h]coumarin (4IPMBC) and 4-(4-iodophenoxymethyl)-6-methoxy-coumarin (4IPMMC) exhibited higher anticancer and antimycobacterial activities [16]. Coumarin molecule exerts diversified nature of interactions (hydrophobic, hydrogen bonds, electrostatics) with many key sites in organisms and therefore it is able to produce wide-range of pharmacological activities. Because of their synthetic versatility, phenylcoumarins (an extra phenyl ring is attached to any position of the coumarin scaffold) are considered as important molecular moiety with proved biological and pharmacological properties [17].

In order to facilitate this synthesis, this paper investigates the molecular origins of the coumarins and studied the photophysical properties and dipole moment of newly synthesised compound using theoretical and experimental techniques.

2 Experimental

2.1 Materials and Methods

Chemicals and reagents used were procured from Sigma Aldrich chemical company, India. Analytical grade solvents were purchased from S.D. Fine Chemicals Ltd. India.

The absorption, fluorescence and fluorescence lifetime measurements were measured using Hitachi U-3310, Hitachi F-7000 and ISS ChronoBH time correlated single photon counting spectrometer.The Melting points of the synthesized compounds were determined by electrothermal apparatus in open capillaries in a Boetius-Mikroheiztisch. TLC was performed by using an aluminium foil fluorescent indicator from Merck KGaA (silica gel 60 F254, layer thickness 0.2 mm). ^{1}H-NMR spectrum was recorded using a Jeol with 100MHz operating frequency deuterated chloroform ($CDCl_3$) solvents. IR spectra were of the dyes recorded using Nicolet 5700 FT-IR instrument.

2.2 Synthesis and characterization of D–π–A substituted bromomethylcoumarinderivatives

In the present work, we described the low-cost and one-step synthesis of some important fluorescent organic bromomethylcoumarin derivatives which are seen to be very important and useful for optoelectronics applications. A mixture of 2-bromosesamol **2**(2.17g, 10 mmol) and anhydrous potassium carbonate (1.38g, 10 mmol) was stirredfor 30 minutes in dry acetone (30 mL). To this, 5,6-Benzo-4-bromomethylcoumarin**1** (2.53g, 10 mmol) was added and the stirring was continued for 24 h. Then, the resulting reaction mixture was poured to crushed ice. The separated solid was filtered and washed with 1:1 HCl (30 mL) and with water. Then product 1-(6-Bromo-benzo[1, 3]dioxol-5-yloxymethyl)-benzo[f]chromen-3-one (1BDYMBC) was recrystallized from ethanol-ethyl acetate (1:1) mixture.

A mixture of 2-bromosesamol **2** (2.17g, 10 mmol) and anhydrous potassium carbonate (1.38g, 10 mmol) was stirred for 30 minutes in dry acetone (30 mL). To this, 7,8-Benzo-4-bromomethylcoumarin **1** (2.53g, 10 mmol) was added and the stirring was continued for 24 h. Then, the resulting reaction mixture was poured to crushed ice. The separated solid was filtered and washed with 1:1 HCl (30 mL) and with water. Then product 4-(6-Bromo-benzo[1, 3]dioxol-5-yloxymethyl)-benzo[h]chromen-2-one (4BDYMBC) was recrystallized from ethanol-ethyl acetate (1:1) mixture.

Their structural identities and purities were confirmed by ^{1}H-NMR, IR and MS and were found to be in good agreement with the proposed structures. The schematic synthesis of bromomethylcoumarin derivatives is shown in Scheme 1–2.

Spectral data of 1BDYMBC

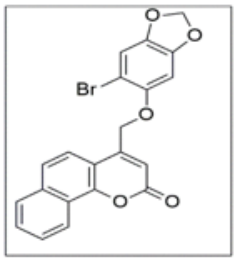

Redsolid,mp:316-318^0**C;**IR(KBr,cm^{-1})1717(C =O),2896(Aliphatic- CH), 3062 (Ar-CH,1086; ^{1}HNMR(400MHz,DMSO,δppm):9.2(s,1H C-H), 8.63(d,1HandAr-H),8.24(t,1HandAr-H),7.92-7.93(m,2H), 7.51(d,1HandAr-H),7.32(d,1HandAr-H),6.9 (s,1HandAr-H).6.4(d,1HandAr-H), 3.7 (s, 1H, aliphatic C-H),2.9 (s, 1H, aliphatic C-H), (LC-MS:427.2(M^{+2}).

Spectral data of 4BDYMBC

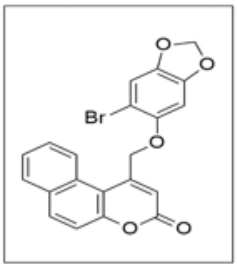

Whitesolid,mp:215-217^0**C;**IR(KBr,cm^{-1})1717(C =O),2894(Aliphatic- CH), 3397 (Ar-CH,1086; ^{1}HNMR(400MHz,DMSO,δppm):9.2(s,1H C-H), 8.72(d,1HandAr-H),8.36(t,1HandAr-H),7.87-7.82(m,2H), 7.63(d,1HandAr-H),7.37(d,1HandAr-H),6.9 (s,1HandAr-H).6.3(d,1HandAr-H), 3.9 (s, 1H, aliphatic C-H),2.6 (s, 1H, aliphatic C-H), (LC-MS:427.2(M^{+2}).

3. Result And Discussions

3.1Estimation of ground and excited-state dipole moments

The absorption and fluorescence spectra of synthesized bromomethyl coumarin fluorescent dyes in different solvents were recorded multiple numbers times in order to check the reproducibility of readings, to avoid any procedural mistakes and the verified spectra are shown in Figs. 1–2. The absorption maxima, emission maxima, Stoke's shift and arithmetic mean of Stoke's shift values in different solvents for all molecules are tabulated in Tables 1–2. The value of the Stokes shift undergoes redshift with an increase in solvent polarity for all the molecules, which indicates $\pi-\pi*$ transition and also suggests that, the dipole moments for all the molecules in the excited state may be higher than the ground state.

When a molecule is excited, the solvent dipoles can reorient or relax around the excited probe molecule and lowers the energy of the excited state. Further, as the solvent polarity increases, this effect becomes larger, which in turn, may result in the emission at lower energies or longer wavelengths. When the molecule is in the excited state, there will be a redistribution of the charges, which may lead to the change in dipole moment [18]. In the excited state, no more the fluorophore remains in equilibrium with its environment. As the molecule relaxes and attains equilibrium with the surrounding environment, some amount of energy is dissipated in the form of non-radiative energy and as a result the fluorescence emission wavelength gets shifted. In addition to this, there may be specific interactions between the probe molecule and solvent like hydrogen-bonding, formation of charge transfer states, complex formation, etc., which may lead to large spectral shifts [18]. Therefore, a systematic analysis of solvent effect is useful in order to understand the effect of the environment and the various mechanisms of deexcitation and relaxation of an excited molecule in solution.

In this regard, the theories developed by various researchers in the field of estimation of ground and excited state dipole moments through solvatochromic methods are used in the present study. The Lippert [19] derived equations based on Onsager's reaction field theory for the determination of dipole moments considering fluorophore as a point dipole in a continuous medium of uniform dielectric constant.

The excited state dipole moments can also be estimated using Bakhshiev [20]and Kawskiet al. [21] have developed a simple quantum mechanical second order perturbation theory to explain absorption and fluorescence band shifts in different solvents of refractive index (N) and varying permittivity (ε_0) corresponding to the band position of a solute molecule.

According to Lippert [19], the expression for Stoke's shift is

$$\bar{\upsilon}_a - \bar{\upsilon}_f = SF(\epsilon, n) + const$$

1

Where $F(\epsilon, n)$ttis Lippert's polarity function and is given by,

$$F(\epsilon, n) = \left[\frac{\epsilon - 1}{2\epsilon + 1} - \frac{n^2 - 1}{2n^2 + 1} \right]$$

2

The expression for Stoke's shift according to Bakhshiev [20] is given by,

$$\bar{\upsilon}_a - \bar{\upsilon}_f = S_1 F_1(\epsilon, n) + const$$

3

Where $F_1(\epsilon, n)t$ is Bakhshiev's polarity function and is given by,

$$F_1(\epsilon, n) = \frac{2n^2 + 1}{n^2 + 2} \left[\frac{\epsilon - 1}{\epsilon + 2} - \frac{n^2 - 1}{n^2 + 2} \right]$$

4

According to Kawski-Chamma-Viallet's [21] equation,

$$\frac{1}{2}\left(\bar{\upsilon}_a + \bar{\upsilon}_f\right) = S_2 F_2(\epsilon, n) + const$$

5

Where $F_2(\epsilon, n)$ is Kawski-Chamma-Viallet's polarity function and is given by

$$F_2(\epsilon, n) = \frac{2n^2 + 1}{2(n^2 + 2)} \left[\frac{\epsilon - 1}{\epsilon + 2} - \frac{n^2 - 1}{n^2 + 2} \right] + \frac{3}{2} \left[\frac{n^4 - 1}{(n^2 + 2)^2} \right]$$

6

Here $\bar{\upsilon}_a$ and $\bar{\upsilon}_f$ are absorption and fluorescence maxima in wave numbers respectively and other terms have their usual meaning.

The dielectric constants, refractive indices, solvent polarity parameter and the calculated values of various polarity functions like F(ε, n), F_1(ε, n) and F_2(ε, n) are given in Table-3.

Dielectric constant (ε), refractiveindex (N), microscopic solvent polarity function (E_T^{tN}) values tare taken from literature [22].

From Eq. 1, .3 and 5, it follows that ($\bar{\upsilon}_a$ - $\bar{\upsilon}_f$) versus F(□, n), ($\bar{\upsilon}_a$ - $\bar{\upsilon}_f$) versus F_1(□, n) and ($\bar{\upsilon}_a$ + $\bar{\upsilon}_f$)/2 versus F_2(□, n) plots should be linear with slopes S, S_1 and S_2 respectively and are given as,

$$S = \frac{2(\mu_e - \mu_g)^2}{hca_0^3}$$

7

$$S_1 = \frac{2(\mu_e - \mu_g)^2}{hca_0^3}$$

8

$$S_2 = \frac{2(\mu_{ett}^2 - \mu_{gt}^2)}{hca_0^3}$$

9

Where μ_e and μ_g are excited and ground state dipole moments respectively. Here the term 'h' is Planck's constant, 'c' is velocity of light in vacuum and 'a_0' is the Onsager cavity radius of the probe molecule and is calculated using Edward's [23] atomic increment method.

The Stoke's shift vs. F(ε, n), Stoke's shift vs. F_1(ε, n) and arithmetic mean of Stoke's shift vs. F_2(ε, n) plots for fluorescent dyes are shown in Fig. 3a-b. The statistical data like slopes, intercepts and correlation coefficients for all molecules are reported in Tables 4. It is observed that, the correlation coefficient values are greater than 0.8, which indicates a good linearity for the slopes S, S_1, and S_2.

Assuming that the symmetry of the probe molecule remains unchanged upon electronic transition and considering the ground and excited state dipole moments to be parallel, the expression for ground state dipole moment (μ_g), excited state dipole moment (μ_e) and ratio of μ_e and μ_g are given by

$$\mu_g = \frac{S_2 - S_1}{2}\left[\frac{hca_0^3}{2S_1}\right]^{1/2}$$

10

$$\mu_e = \frac{S_1 + S_2}{2}\left[\frac{hca_0^3}{2S_1}\right]^{1/2}$$

11

$$\frac{\mu_e}{\mu_g} = \frac{S_1 + S_2}{S_2 - S_1};\ (S_2 > S_1)\ (12)$$

Using the slopes S_1 and S_2, the values of μ_g, μ_e and their ratio μ_e/μ_g were calculated according to Eqs. 10, 11 & 12 and the results are given in Tables 5 and6. Further, by substituting the value of μ_g calculated from Eq. 10, the excited state dipole moment (μ_e)is calculated according to Lippert's, Bakhshiev's and Kawski-Chamma-Viallet's method i.e. from Eqs. 7, 8 & 9 respectively and the results are presented in Table 4.

If the angle between ground and excited state dipole moments are not parallel, then the angle θ between the two dipole moments is determined from the following equation.

$$\cos\theta = \frac{1}{2\mu_g\mu_e}\left[\left(\mu_g^2 + \mu_e^2\right) - \frac{S_2}{S_3}\left(\mu_e^2 - \mu_g^2\right)\right]$$

13

The angle between ground and excited state dipole moments is calculated according to Eq. 13 and the results are presented in Table 5.

3.2 Change in dipole moment (Δμ) and excited state dipole moment (μ_e) by solvent polarity parameter (E_T^N) :

This method is based on solvent polarity parameter $\left(E_T^N\right)$ to estimate change in dipole moment (Δμ)proposed by Reichardt [24]and developed by Ravi et. al.[25]. In this method, the problem associated with the estimation of Onsager cavity radius has been minimized.

The expression for Stoke's shift according to Reichardt and Ravi et a. is,

$$\bar{\upsilon}_a - \bar{\upsilon}_f = 11307.6\left[\left(\frac{\Delta\mu}{\Delta\mu_B}\right)^2\left(\frac{a_B}{a}\right)^3\right]E_T^N + \text{const}$$

14

where $\Delta\mu_B$ (= 9D) and a_B (= 6.2 Å) are the change in dipole moment on excitation and Onsager cavity radius of reference betaine dye molecule and Δμ and 'a' are the change in dipole moment and molecular radius of the molecule under investigation.

The change in dipole moment (Δμ) is determined from the following equation.

$$\Delta\mu = \mu_e - \mu_g = \sqrt{\frac{m \times 81}{\left(\frac{6.2}{a_o}\right)^3 11307.6}}$$

15

Where m is the slope obtained from the linear plot of Stoke's shift versus$\left(E_T^N\right)$.

Then by using Eq. 15 and knowing the value of μ_g (From Eq. 10), the excited state dipole moment is determined from the following equation.

$$\mu_e = \Delta\mu + \mu_g$$

16

The relevant plots of Stoke's shift vs.$\left(E_T^N\right)$ required for the determination of change in dipole moment (Δμ) for all the probe molecules are shown in Fig. 3a-b. Using the slopes calculated from Stoke's shift versus E_T^N, the excited state dipole moment (μ_e) and change in dipole moment (Δμ) for both the molecules were calculated using Eq. 16 and the results are presented in Table 5–6.

The ground state dipole moment of 4BDYMBCis higher as compared to 1BDYMBCand it may be due to the substitution of benzene in coumarin moiety due to more electro negativitywhich create decreases the bond length and increases polarizability, which may lead to the increase in the dipole moment [26]. It is also observed from Table-5 that, the excited state dipole moment (μ_e) for the molecule 1BDYMBC is less than the 4BDYMBC. The decrease of excited state dipole moment (μ_e) for the molecule 1BDYMBC may suggest different geometry for the singlet excited state than remaining molecules, indicating a significant difference in the charge distribution.

The excited state dipole moment (μ_e) determined by using Bakhshiev's, KawskiChamma-Viallet's, and solvatochromic eqns. (Table-5) were found to be in good agreement with each other. The higher values of excited state dipole moment (μ_e) observed in case of Lippert's method compared to other methods may be due to the non-accountability of polarizability. However, μ_e calculated by using solvent polarity parameter E_T^N (Eq. 6) is found to be smaller than μ_e determined from Bakhshiev's, Kawski-Chamma-Viallet's and solvatochromic methods. This may be due to the reason that these methods do not consider specific solute-solvent interactions like hydrogen bonding, complex formation and molecular aspects of solvation, whereas they are incorporated in the solvent polarity parameter [27].

The μ_e values are found to be higher than μ_g values for all the molecules (Table 5). The higher values of μ_e indicate that the probe molecules are more polar in the excited state than the ground state. The angle between ground and excited state dipole moment for both the molecules are found to be zero degree which suggest that, μ_g and $\mu_e$are parallel to each other and the molecular symmetry remains same upon electronic transition [27]. Further, it is observed that the change in dipole moment ($\Delta\mu$) value is found to be higher. The higher values of $\Delta\mu$ may indicate the existence of more relaxed excited state and which may be due to ICT. The possible intramolecular charge transfer may be attributed to the resonance structures of synthesized molecule and are shown in Fig. 4a-b.

3.3. Computational analysis

The absorption and emission spectra of all molecules in different solvents were computed by using Gaussian 09W in order to compare with the experimental results. For this purpose, the molecule is optimized for the ground and excited state using DFT and TD-DFT with the basis sets B3LYP/3-211G combined with integral equation formalism variant-Polarizable Continuum Model (IEFPCM) solvation model.

The ground-state dipole moment of the probe molecule in the gaseous state is also estimated theoretically by using DFT with basis sets B3LYP/3-11G and the result is presented in Table 7. The optimized molecular geometry of all molecules along with the direction of dipole moment is shown in Fig. 5.

It is observed from Tables6-7 that the theoretically computed μ_g value is higher than the experimental μ_g value. It is to be noted that the experimental methods take solvent and environmental effects like solute-solvent interactions into account, whereas the ab initio computations are based on gaseous phase [28–30]. Further, in order to analyze the solute-solvent interactions, the ground dipole moments are estimated theoretically for all the studied solvents by using IEF-PCM solvation model and the results are given in Table 8 and it is noticed that the ground-state dipole moment values for each of the solvents are found to be higher than the ground-state dipole moment value of the probe molecule in the gaseous phase. The increase in the dipole moment value is due to the consideration of environmental effects like solute-solvent interactions in the IEF-PCM solvation model. Further, the excited-state dipole moment values were found to be higher than the corresponding ground-state dipole moment values for all the solvents and this suggests that the probe molecule is more polar in the excited state than the ground state. It is interesting to note that the computational studies also reproduce the similar trend as observed experimentally. However, the theoretically computed ground- and excited-state dipole moments were found to be higher than the experimental dipole moments.

The 3D plots of HOMO and LUMO of synthesized fluorescent dye are shown in Fig. 6. The HOMO, LUMO energies and HOMO-LUMO energy band gap (ΔE) value for the probe molecule are presented in Table 7.

The optical band gap E^{opt}_{g} is determined from absorption threshold wavelength for both molecules and the results are tabulated in Table 8. It is observed that the HOMO-LUMO energy band gap is in order with the experimental optical energy band gap. The lower values of energy gap for the probe molecule also support the observed higher values of excited-state dipole moments. The determination of HOMO-LUMO energies also helps in understanding the chemical stability of a molecule in terms of a parameter known as chemical hardness (η). The molecules possessing large HOMO-LUMO energy gap are considered as hard, whereas moleculespossessing small HOMOLUMO energy gaps are considered as soft molecules [31–32]. The chemical hardness (η) of a molecule is determined from Eq. 17.

$$\eta = \frac{E_L - E_H}{2}$$

17

where E_H and E_L are the HOMO and LUMO energies

The chemical hardness (η) estimated for all fluorescent dyes and are given in Table 8. The small values of chemical hardness (η) and HOMO-LUMO energy gaps suggest that the molecule may be considered as soft molecule. These results also support the observed higher values of μ_e.

The molecular electrostatic potential (MESP) plots provide the information for determining a suitable position for nucleophilic and electrophilic attack along with the hydrogen bonding interactions of solvent. The MESP 3D plot shown in Fig. 7.

In this plot, different colors correspond to different values of electrostatic potential at the surface. The red color represents negative phase, which can be related to the electrophilic site, and blue color represents positive phase, which corresponds to nucleophilic site. From Fig. 7, it is observed that the MESP plot of all molecule shows negative phases around 3H-benzo[f]chromen-3-onewhereas positive phases around all hydrogen atoms.

4. Conclusion

In the present studies, we have synthesizeda D-π-A substituted bromomethylcoumarinderivatives via one-pot chemical reaction. The ground state dipole moments of fluorescent dyes are estimated theoretical and experimental methods. The result shows that the theoretical ground state dipole moments (μ_g) values are higher than the experimental ground state dipole moments values. Further, It is observed that the excited state dipole moments (μ_e) determined from Bakhshiev's, Kawski-Chamma-Viallet's, solvatochromic equation are found to be in good agreement with each other. Further, the excited state dipole moments determined from all the methods are found to be higher than the ground state dipole moments for all molecules under investigation and this suggest that the fluorescent dyes are more polar in the excited state than in the ground state. It is observed that the angle between μ_g and μ_e all molecules are found to be zero degree, which suggests that, μ_g and $\mu_e$is parallel to each other and there is no change in the symmetry upon electronic transition. The HOMO-LUMO energy band gaps determined from DFT computations and also from optical energy band gaps using absorption threshold wavelengths are found to be in good agreement. Using HOMO-LUMO energies, the chemical hardness of the molecules is studied and the results suggest that all the molecules exhibit the soft nature. The computational studies performed using DFT calculations imply that the fluorescent dyes exhibit both nucleophilic and electrophilic sites. These preliminary observations and results suggest that, the fluorescent dyes may be considered as potential and interesting fluorescent probes for luminescence materials, fluorescent probes and for dye sensitized solar cell materials in future.

Declarations

Acknowledgment: The author Mahesh Madar acknowledges to the technical staff of USIC, Karnatak University, Dharwad for recording the data of absorption and emission spectra. The author is also grateful to the Principal, Teaching & Non-teaching staff, and Management of V.M.K. S.R.Vastrad College Hungund.

Author Contributions: Mahesh Madar: Characterization of derivative, experimental planning and studies, data analysis, major work in draft writing. **Shridhar A. H.:** Computational analysis, theoretical ground state, and dipole moment calculation, energy HUMO and LUMO estimation. **M. Basanagouda:** Synthesis of D-PI-A subst.... bromo.... derivative, planning of work spectral data analysis. **M. S. Pujar:** Planning of work, statistical data analysis, draft editing, and final proofreading. **A. H. Sidarai:** Language editing and overall review work administration.

Funding: The authors declare that no funds, grants were received during the preparation of this manuscript.

Data Availability: All data generated or analyzed during this study are included in this published article.

Ethical Approval: This article does not contain any studies with human or animal subjects.

Informed Consent: A statement regarding informed consent is not applicable.

Conflict of Interest: All authors, Mahesh Madar, Malatesh S. Pujar, Shridhar A. H., Mahantesh M. Basanagouda, Ashok H. Sidarai are declare no conflict of interest.

Consent to participate: Not applicable.

Consent to publication: Not applicable.

Code availability: Not applicable.

References

1. Pope M, Swenberg C (1999) Electronic Processes in Organic Crystals and Polymers. Oxford Science Publication
2. Kohler A, Bassler H (2015) Electronic Processes in Organic Semiconductors. Weinheim, Germany, Wiley-VCH Verlag GmbH & Co. KGaA
3. Cicoira F, Santato C (2013) Organic Electronics: Emerging Concepts and Technologies. Wiley-VCH
4. Lanzani G (2012) The Photophysics behind Photovoltaics and Photonics. Wiley-VCH
5. Katerinopoulos HE (2004) Curr Pharm Des 30:3835. doi:10.2174/1381612043382666
6. Dandriyal J, Singla R, Kumar M, Jiatak V (2016) Eur J Med Chem 119:141. doi:10.1016/j.ejmech.2016.03.087
7. Zhang H, Luo Q, Mao Y, Zaho Y, Yu T (2017) J PhotochemPhotobiolA Chem 346:10. doi:10.1016/j.jphotochem.2017.05.039
8. Garcia S, Vazquez JL, Renteria M, Gurduno IGA, Delgado F, Duran MJ, Revilla MAG, Mendez EA, Vazquez MA (2016) Opt Mater 62:231. doi:10.1016/j.optmat.2016.09.065
9. Hara K, Sayama K, Ohga Y, Shinpo A, Saga S, Arakawa H (2001) Chem Commun 6:69. doi:10.1039/B010058G
10. Merlo AA, Tavares A, Khan S, Santos MJL, Teixeira SR (2018) Liq Cryst 45:310. doi:10.1080/02678292.2017.1324644
11. Tasior M, Poronik YM, Vakuliuk O, Sadowski B, Karczewski M, Gryko DT (2014) J Org Chem 79:8723. doi:10.1021/jo501565r
12. Borges F, Roleira F, Milhazes N, Santana L, Uriarte (2005) E. Simple coumarins and analogues in medicinal chemistry: Occurrence, synthesis and biological activity. Curr. Med. Chem., 12, 887–916
13. Anand P, Singh B, Singh N (2012) A review on coumarins as acetylcholinesterase inhibitors for Alzheimer's disease. Biorg Med Chem 20:1175–1180
14. Kulkarni MV, Pujar BJ, Patil VD (1983) Arch Pharm 316:15–21
15. Vasudevan KT, Kulkarni MV, Pauutaraja (1994) Acta Crystallogr. C50, 1286–1288
16. Basanagouda M, Jambagi VB, Barigidad NN, Laxmeshwar SS, Devaru,Narayanachar V (2014) Eur J Med Chem 74:225–233

17. Stefanachi A, Leonetti F, Pisani L, Catto M, Carotti A (2018) Coumarin: A Natural, Privileged and Versatile Scaffold for Bioactive Compounds. Molecules 23:250
18. Mataga N, Kaifu Y, Koizumi M (1956) Solvent effects upon fluorescence spectra and the dipole moments of excited molecules. Bull Chem Soc Jpn 29:465–470. doi:https://doi.org/10.1246/bcsj.29.465
19. Lippert EZ (1957) Spektroskopische bestimmung des dipolmomentes aromatischer verbindungen im ersten angeregten singulettzustand. Z Elektrochem 61:962–975. doi:10.1002/bbpc.19570610819
20. Bakhshiev NG, Bakhshiev NG (1964) Universal intermolecular interactions and their effect on the position of the electronic spectra of molecules in 2-component solutions. Opt Spectrosc 16:821–832
21. Kawski A (2002) On the estimation of excited state dipole moments from solvatochromic shifts of absorption and fluorescence spectra. Z Naturforsch 57A:255–262. doi: https://doi.org/10.1515/zna-2002-0509
22. Parkanyi C, Aaron JJ (1998) Dipole moments of aromatic heterocycles, theoretical and computational Chemistry, 5, 233–258
23. Edward JT (1970) Molecular volumes and the Stokes-Einstein equation. J Chem Educ 47:261–270. doi:https://doi.org/10.1021/ed047p261
24. Reichardt C (1994) Solvatochromic dyes as solvent polarity indicators. Chem Rev 94:2319–2358. doi:https://doi.org/10.1021/cr00032a005
25. Ravi M, Soujanya T, Samanta A, Radhakrishnan TP (1995) Excited state dipole moments of some coumarin dyes from a solvatochromic method using the solvent polarity parameter. J Chem Soc Faraday Trans 91:2739–2742. doi:https://doi.org/10.1039/FT9959102739
26. Smith MB, March J (2012) March's Advanced Organic Chemistry: Reaction, Mechanisms and Structure, sixth edn. Wiley, New York
27. Maridevarmath CV, Naik L, Negalurmath VS, Basanagouda M, Malimath GH (2019) Synthesis, characterization and photophysical studies on novel benzofuran-3-acetic acid hydrazide derivatives by solvatochromic and computational methods. J Mol Struct 1188:142–152
28. Aaron JJ, Maafı M, Kersebet C, Parkanyi C, Antonious MS, Motohashi N (1996) A solvatochromic study of new benzo[a]phenothiazines for the determination of dipole moments and specific solute-solvent interactions in the first excited singlet state. J Photochem Photobiol A 101:127–136. doi: https://doi.org/10.1016/S1010-6030(96)04442-5
29. Adenier A, Aaron JJ, Parkanyi C, Deng G, Sallah M (1996) Solvent effects on the electronic absorption and fluorescence emission spectra of merocyanine 540 - a biological probe. Heterocycl Commun 2(5):403–408
30. Sidir YG, Sidir I (2013) Solvent effect on the absorption and fluorescence spectra of 7-acetoxy-6-(2,3-dibromopropyl)-4,8-dimethylcoumarin: Determination of ground and excited state dipole moments,Spectrochim. Acta A Mol Biomol Spectrosc 102:286–296
31. Akshaya KB, Anitha V, Prajwal LL, Rekakumari G, Louis (2016) Synthesis and photophysical properties of a novel phthalimide derivative using solvatochromaic shift method for the estimation of ground and singlet excited state dipole moments. J Mol Liquids 224:247–254
32. Roshmy A, Anita V, Louis G, Aatika N (2016) Estimation of ground state and excited state dipole moments of a novel Schiff base derivative containing 1,2,4-triazole nucleus by solvatochromic method. J Mol Liq 215:387e395

Tables

1. Spectroscopic data of 1BDYMBCin different solvents

Solvent	λ_a (nm)	λ_f (nm)	$\bar{\nu}_a$[a] (cm^{-1})	$\bar{\nu}_f$[b] (cm^{-1})	$(\bar{\nu}_a - \bar{\nu}_f)$[c] ($cm^{-1}$)	$\frac{(\bar{\nu}_a + \bar{\nu}_f)}{2}$[d] ($cm^{-1}$)
Benzene	331	418	30211	23923	6288	27067
Toluene	332	420	30120	23810	6311	26965
DEE	333	421	30030	23753	6277	26891
Ethyl acetate	335	423	29851	23641	6210	26746
Methyl chloride	336	424	29762	23585	6177	26673
Isoproponol	339	426	29499	23474	6024	26486
Acetone	340	428	29412	23364	6047	26388
Ethanol	341	429	29326	23310	6015	26318
Methanol	341	434	29326	23041	6284	26183
DMF	342	436	29240	22936	6304	26088
Acetonitrile	346	440	28902	22727	6174	25815
DMSO	347	418	30211	23923	6288	27067

[a]Absorption maxima; [b]Fluorescence maxima; [c]Stokes shift; [d]Arithmetic mean of absorption maxima and fluorescence maxima.

2. Spectroscopic data of 4BDYMBC in different solvents

Solvent	λ_a (nm)	λ_f (nm)	$\bar{\nu}_a$[a] (cm^{-1})	$\bar{\nu}_f$[b] (cm^{-1})	$(\bar{\nu}_a - \bar{\nu}_f)$[c] ($cm^{-1}$)	$\frac{(\bar{\nu}_a + \bar{\nu}_f)}{2}$[d] ($cm^{-1}$)
Benzene	333	405	30030	24691	5339	27361
Toluene	334	407	29940	24570	5370	27255
DEE	335	412	29851	24272	5579	27061
Ethyl acetate	336	415	29762	24096	5666	26929
Methyl chloride	336	417	29762	23981	5781	26871
Isoproponol	337	421	29674	23753	5921	26713
Ethanol	341	423	29326	23641	5685	26483
Methanol	342	423	29240	23641	5599	26440
DMF	343	424	29155	23585	5570	26370
Acetonitrile	343	424	29155	23585	5570	26370
DMSO	344	440	29070	22727	6342	25899

[a]Absorption maxima; [b]Fluorescence maxima; [c]Stokes shift; [d]Arithmetic mean of absorption maxima and fluorescence maxima.

3. Physical constants along with the calculated values of various polarity functions.

Solvent	ε	N	E_T^N	F(ε,n)	F_1(ε,n)	F_2(ε,n)
Benzene	2.27	1.558	0.111	0.014	0.033	0.715
Toluene	2.40	1.496	0.099	0.015	0.033	0.703
Ethyl acetate	6.02	1.372	0.228	0.199	0.489	0.995
THF	7.58	1.407	0.207	0.209	0.549	1.102
Dichloromethane	8.93	1.424	0.321	0.217	0.590	1.165
Isopropanol	20.45	1.380	0.546	0.276	0.781	1.298
Acetone	20.70	1.359	0.355	0.284	0.790	1.279
Ethanol	24.30	1.361	0.654	0.288	0.811	1.303
Methanol	33.70	1.328	0.762	0.309	0.857	1.304
Acetonitrile	37.50	1.346	0.46	0.304	0.862	1.333
DMF	38.25	1.430	0.386	0.275	0.839	1.422
DMSO	47.24	1.479	0.444	0.263	0.841	1.488

4. Statistical treatment of the correlations of solvents spectral shifts of fluorophores

Molecule	Correlations	Slope (cm^{-1})	Intercepts (cm^{-1})	Correlation coefficient	No. of data
1BDYMBC	Lippert's –Mataga correlation	1814(S_1)	5991	0.939	6
	Bakhshiev's correlation	561(S_2)	5871	0.948	5
	Kawski-Chamma-Viallet's correlation	-2509 (S_3)	28064	0.964	7
	Reichardt's correlation	650(m)	6093	0.901	5
4BDYMBC	Lippert's –Mataga correlation	1580(S_1)	5353	0.939	6
	Bakhshiev's correlation	225(S_2)	5186	0.935	5
	Kawski-Chamma-Viallet's correlation	-2739 (S_3)	28339	0.907	10
	Reichardt's correlation	1286(m)	5286	0.928	6

5. Ground and Excited state dipole moment values of synthesized compounds

				Excited State Dipole moment μ_e(D) according to				
Molecule	Radius (Å)	Theoretical Ground State Dipole Moment μ_g(D)	Ground State Dipole Moment μ_g(D)	Lippert	Bakhshiev	Kawski-Chamma-Viallet	Solvatochromic method	Solvent Polarity Parameter
1BDYMBC	4.212	6.427	3.543	7.212	5.583	5.583	5.583	4.904
4BDYMBC	4.212	7.003	7.219	10.657	8.512	8.512	8.512	9.141

6. Change in dipole moment, ratio and angle between μ_e & μ_g

Molecule	Change in Dipole moment (Δμ) (D) from		Ratio of Excited & Ground state dipole moment	Angle between μ_g&μ_e
	Solvatochromic Method	Solvent Polarity Parameter	μ_e/μ_g	θ in Degree
1BDYMBC	2.041	1.366	1.576	0
4BDYMBC	1.292	1.922	1.176	0

7. Theoretical ground state dipole moment (m_g) in different solvents

Solvent	1BDYMBC				4BDYMBC			
	μ_g (D)	HOMO eV	LUMO eV	DE eV	μ_g (D)	HOMO eV	LUMO eV	DE eV
Benzene	7.442	-6.022	-2.088	3.934	8.012	-6.179	-2.288	3.891
Toluene	7.531	-6.023	-2.101	3.922	8.223	-6.142	-2.269	3.873
DEE	7.664	-6.021	-2.159	3.862	8.984	-6.019	-2.276	3.743
Ethyl acetate	7.745	-6.018	-2.206	3.812	9.145	-6.013	-2.302	3.711
Methyl chloride	7.843	-6.026	-2.245	3.781	9.267	-5.999	-2.308	3.691
Isoproponol	7.912	-6.014	-2.235	3.779	9.395	-5.901	-2.229	3.672
Ethanol	7.993	-6.011	-2.245	3.766	9.591	-5.891	-2.338	3.553
Methanol	8.052	-5.999	-2.265	3.734	9.697	-5.888	-2.467	3.421
DMF	8.112	-5.983	-2.317	3.666	9.823	-5.845	-2.506	3.339
Acetonitrile	8.213	-5.981	-2.325	3.656	9.862	-5.811	-2.487	3.324
DMSO	8.304	-5.977	-2.466	3.511	9.877	-5.766	-2.654	3.112

8. Chemical hardness (η), Energy of HOMO and LUMO, Energy gap (Δ *E*)of the fluorophores in ethanol and experimentally estimated optical energy band gap (E_g^{opt})

Molecule	E_{HOMO} (eV)	E_{LUMO} (eV)	ΔE	(eV)	E_g^{opt} (eV)	η (eV)
1BDYMBC	-6.109	-2.088	4.021		3.746 (at 331 nm)	2.010
4BDYMBC	-5.992	-1.907	3.985		3.724 (at 333 nm)	1.992

Scheme

Scheme 1 is available in Supplementary Files section.

Figures

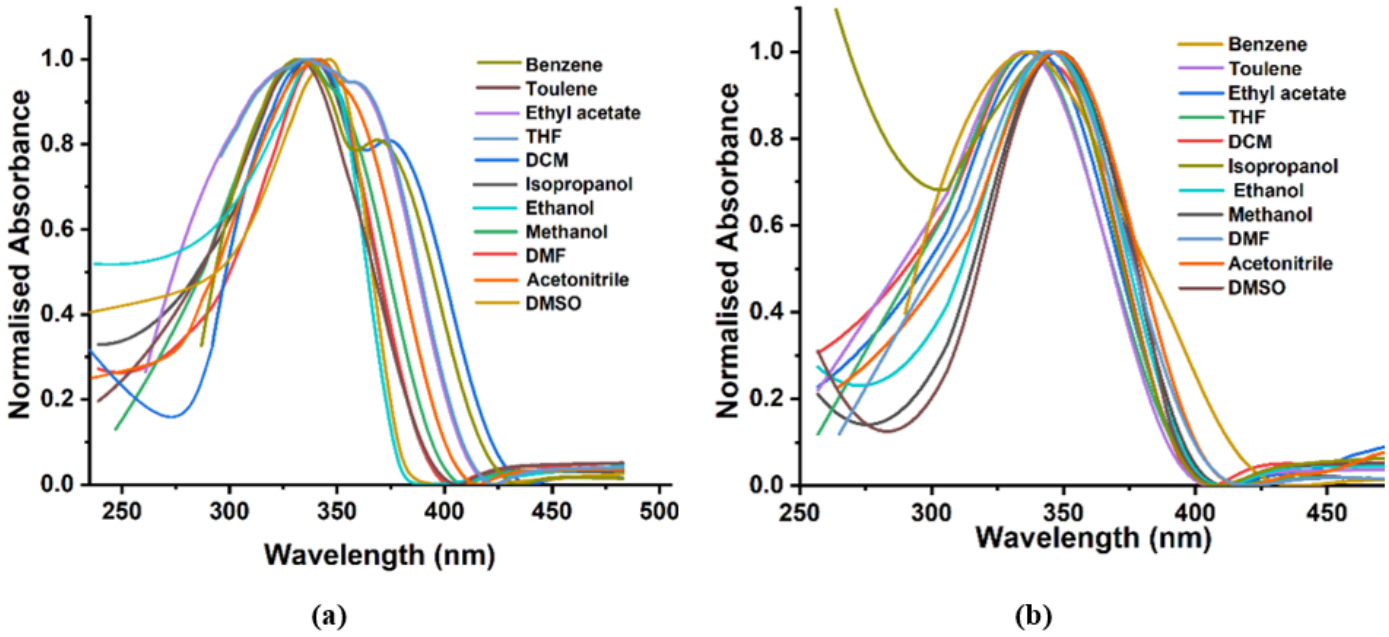

Figure 1

Absorption spectra of (a) 1BDYMBC and (b) 4BDYMBC in different solvents

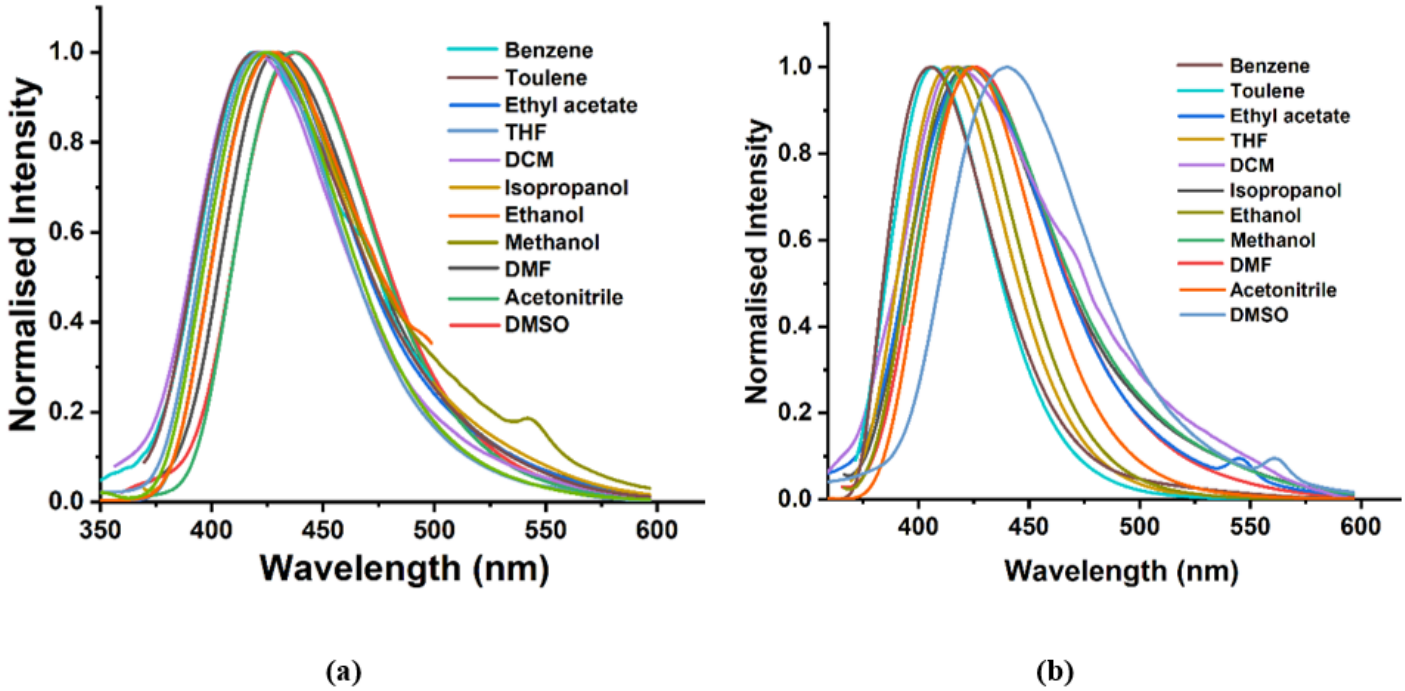

Figure 2

Fluorescence spectra of (a) 1BDYMBC and (b) 4BDYMBC in different solvents

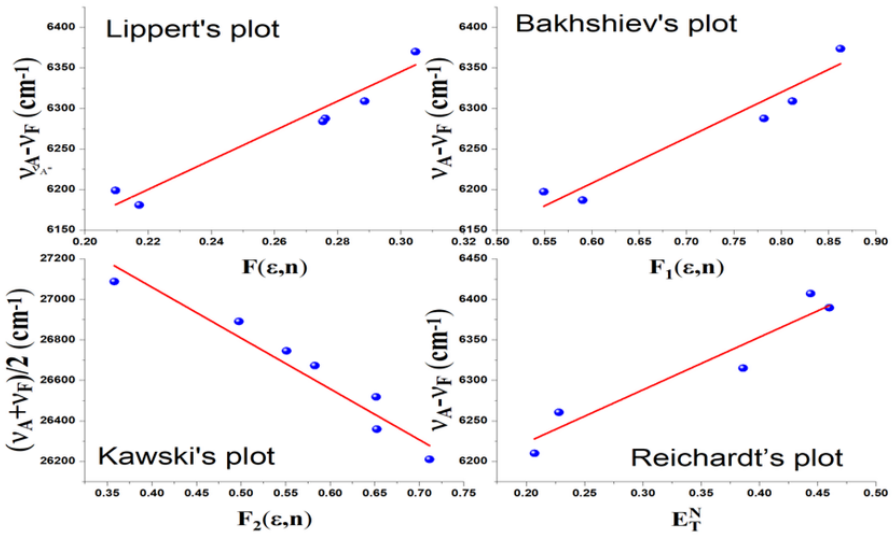

A

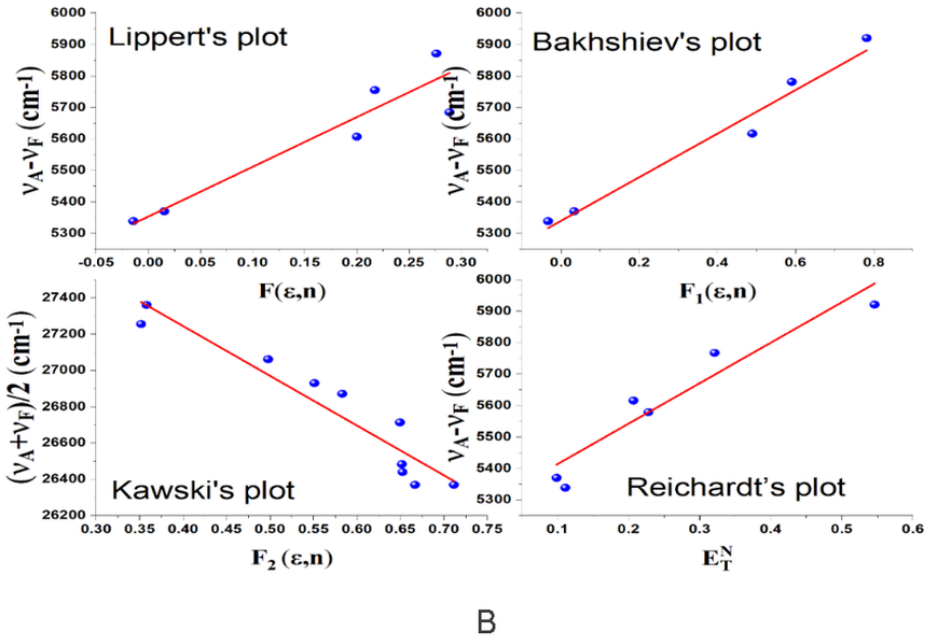

B

Figure 3

a Lippert's-Mataga, Bakhshiev's, Kawski-Chamma-Viallet, and Reichardt's plots for 1BDYMBC

b Lippert's-Mataga, Bakhshiev's, Kawski-Chamma-Viallet, and Reichardt's plots for 4BDYMBC

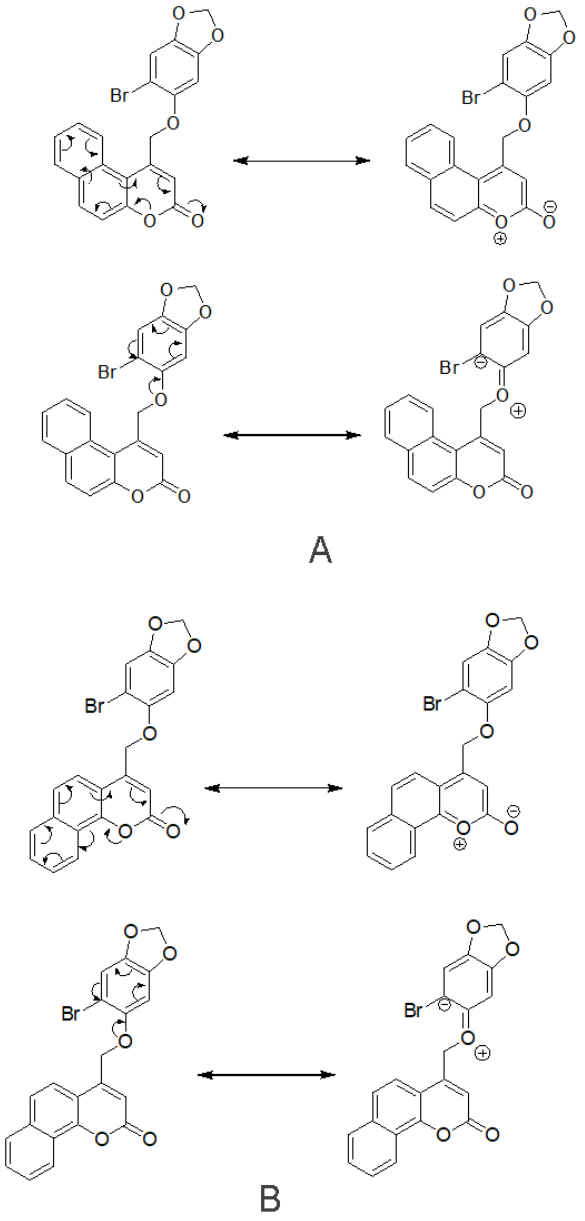

Figure 4

a Possible resonance structures of 1BDYMBC.

b Possible resonance structures of 4BDYMBC.

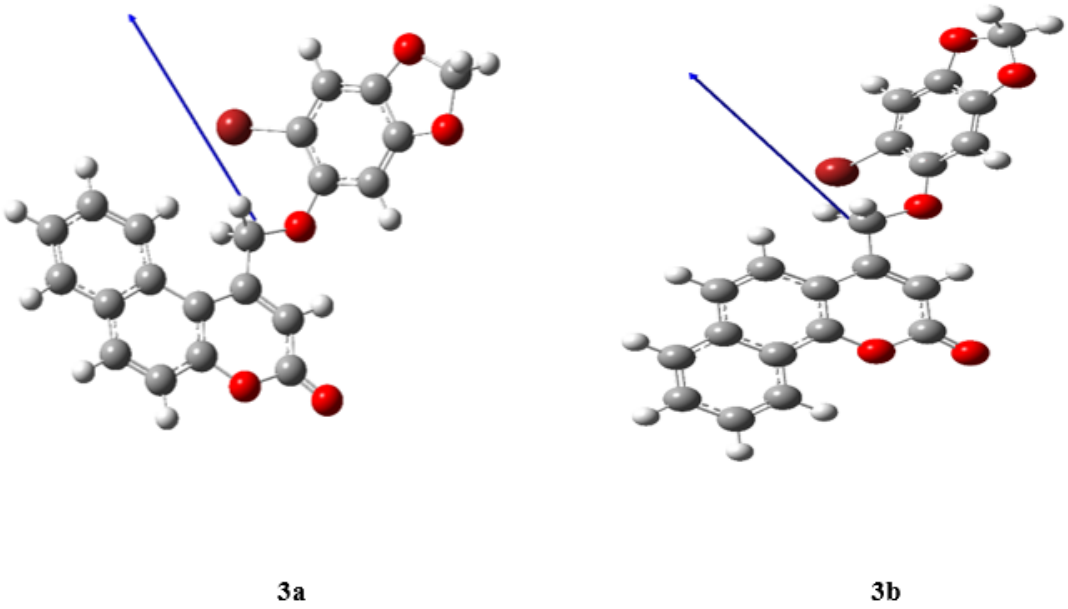

Figure 5

Ground-state optimized molecular geometries of fluorescent dyes. The arrow mark indicates the direction of dipole moment

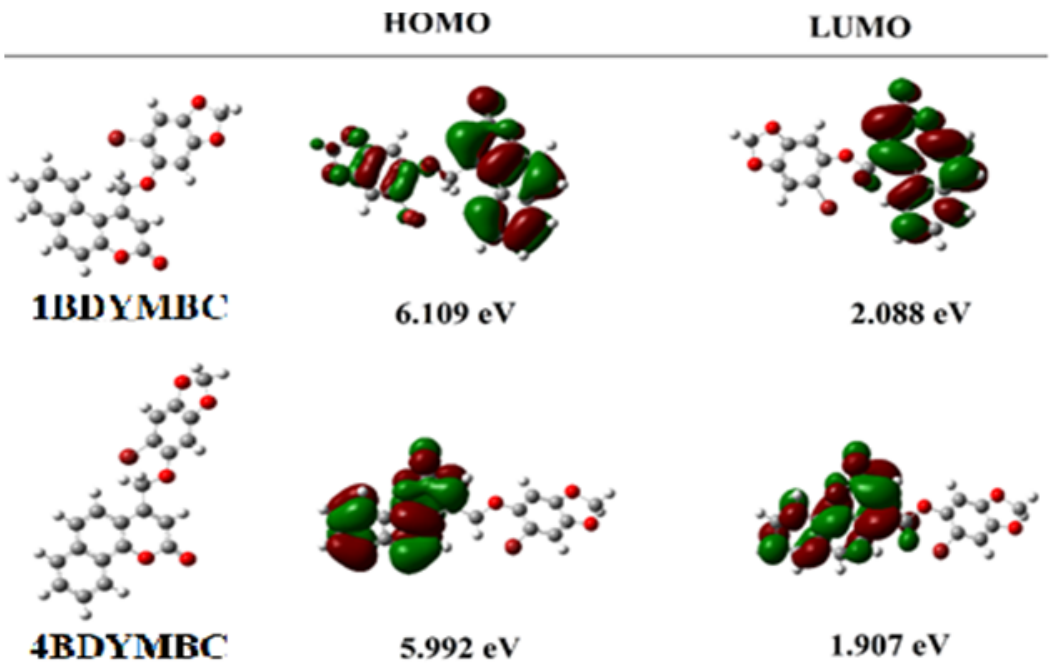

Figure 6

3D plots of HOMO-LUMO with energy levels for 3a-3b

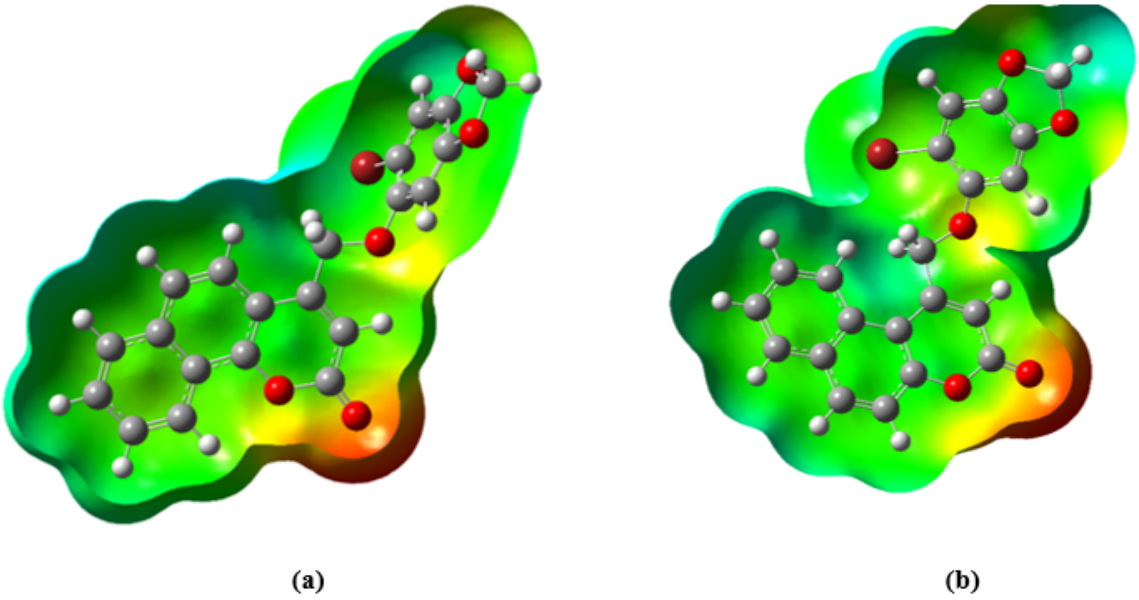

Figure 7

Molecular electrostatic potential (MESP) plots of (a) 1BDYMBC and (b) 4BDYMBC

Supplementary Files

This is a list of supplementary files associated with this preprint. Click to download.

- Scheme1.png